



HAL
open science

Wavenumber-frequency analysis of the wall pressure fluctuations in the wake of a rear view mirror using a lattice Boltzmann model

François van Herpe, Sandrine Vergne, Eric Gaudard

► **To cite this version:**

François van Herpe, Sandrine Vergne, Eric Gaudard. Wavenumber-frequency analysis of the wall pressure fluctuations in the wake of a rear view mirror using a lattice Boltzmann model. *Acoustics* 2012, Apr 2012, Nantes, France. hal-00810780

HAL Id: hal-00810780

<https://hal.science/hal-00810780>

Submitted on 23 Apr 2012

HAL is a multi-disciplinary open access archive for the deposit and dissemination of scientific research documents, whether they are published or not. The documents may come from teaching and research institutions in France or abroad, or from public or private research centers.

L'archive ouverte pluridisciplinaire **HAL**, est destinée au dépôt et à la diffusion de documents scientifiques de niveau recherche, publiés ou non, émanant des établissements d'enseignement et de recherche français ou étrangers, des laboratoires publics ou privés.



ACOUSTICS 2012

Wavenumber-frequency analysis of the wall pressure fluctuations in the wake of a rear view mirror using a lattice Boltzmann model

F. A. Van Herpe^a, S. Vergne^a and E. Gaudard^b

^aPSA PEUGEOT CITROËN, Case Courrier VV1405, Centre Technique de Vélizy A - Route de Gisy, 78140 Velizy Villacoublay, France

^bUPMC-IJLRDA(UMR 7190), 4, Place Jussieu, Cedex 05, 75252 Paris, France
gaudard@dalembert.upmc.fr

An emerging method for the numerical prediction of the wind noise inside a car is the coupling of an unsteady Computational Fluid Dynamics (CFD) solver to a Statistical Energy Analysis (SEA) solver. This approach requires the separation between the aerodynamic and the acoustic components of the Wall Pressure Fluctuations (WPF) loading the car greenhouse panels. Those two components correspond indeed in SEA to two different paths of sound transmission: the structure-borne path and the air-borne path. It has been recently shown using Direct Noise Computation that a wavenumber-frequency Fourier transform of the WPF allows separating the convective aerodynamic component from the propagating acoustic component. We investigate in this paper the ability of the Lattice Boltzmann based CFD code PowerFLOW to capture the low level acoustic component of the WPF in the wake of a rear view mirror over a flat panel. We compare two options in the simulated Mach number setting: The default mode where the Mach number is chosen by PowerFLOW as high as it can in order to reduce the simulation time, and the mode where the simulated Mach number is chosen so that acoustic waves propagate at the same speed as they do in experiment.

1 Introduction

Since other sources of noise (engine, transmission and tires) have been significantly quieted in the last decades, interior wind noise is more than ever a major problem for car manufacturers, especially at highway speed and high frequencies (above 400Hz). Until recent years however, wind noise was only assessed at the end of the car design process, when prototype vehicles were available for wind tunnel tests. The risk of late detection of wind noise problems leading to expensive late design changes, together with the high cost of wind tunnel sessions, have been strong motivations for the development of a computational approach in order to reduce the car development time and the associated costs. The ever extending capabilities of unsteady Computational Fluid Dynamics (CFD) have made this numerical approach nowadays possible.

An emerging method for the numerical prediction of the wind noise inside a car is the coupling of an unsteady CFD solver to a vibro-acoustic Statistical Energy Analysis (SEA) solver [1,2]. This approach requires the separation between the aero-elastic and the acoustic components of the Wall Pressure Fluctuations (WPF) loading the car greenhouse panels. Those two components correspond indeed in SEA to two different paths of sound transmission: the structure-borne path and the air-borne path. It has been recently shown [3] using Direct Noise Computation (DNC) that a wavenumber-frequency Fourier transform of the WPF allows separating the convective aerodynamic component (pseudo sound) from the propagative acoustic component (sound) : Because the sound velocity c_0 is much larger than the pseudo-sound convection velocity U_c for highly subsonic automotive flow, the convective wavenumber $k_c = \omega/U_c$ is much larger than the acoustic wavenumber $k_0 = \omega/c_0$, and they correspond to two distinct peaks on a wavenumber-frequency diagram of the WPF Power Spectral Density (PSD).

By default, the Lattice Boltzmann based CFD code PowerFLOW runs the simulations at a Mach number M as high as possible in order to speed up the calculations. PowerFLOW exploits the fact for low Mach numbers ($M < 0.4$), as long as the Reynolds number is the same, flow results are usually independent of Mach numbers. This might be an awkward choice for simulations where the speed of acoustic waves is important. By setting the simulated Mach number to a greater value, PowerFLOW reduces the apparent speed of sound relative to the main flow speed. We investigate in this paper the influence of the simulated Mach number setting on the WPF computed by PowerFLOW. We compare the default choice where the Mach number is “chosen by PowerFLOW” to the mode

where the Mach number is defined by users as the “same as experiments”.

2 Numerical setup

We focus on the semi-academic case that has already been simulated by DNC [3] because experimental data are available for our calculations’ validation: WPF over a flat panel in the wake of a car rear view mirror.

First the CAD surface of the side mirror has to be meshed using a facetization sufficiently fine to represent its complex geometry. This mesh is used to define the surface elements (surfels) of the simulation grid (lattice) that occur where the surface of a body intersects the fluid.

The Fluid mesh is composed of cubic volume elements (voxels) and is divided into regions of Variable Resolution (VR). VR regions allow for grid refinement or coarsening by a factor of 2. The size of a voxel in the highest level is the finest and the voxel size in the next level down is exactly twice that size. In our PowerFLOW simulations, 10 VR levels were used: Voxels in VR 10 are 2mm on a side, VR 9 voxels are 4mm, VR 8 voxels are 8 mm and so on.

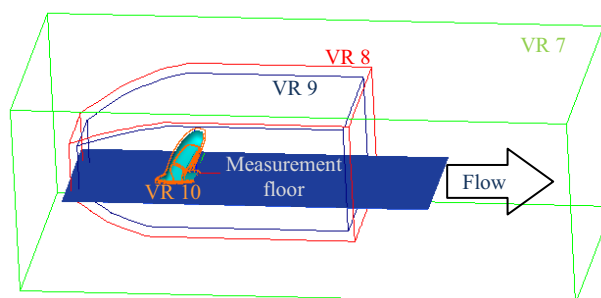


Figure 1: VR regions 10 to 7

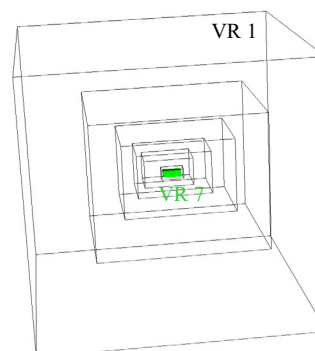


Figure 2: VR setup

Once the VR regions are defined, the fluid mesh is generated automatically. The lattice was finally made of 54 million voxels and 2 million surfels.

The Mach number M at which a simulation is performed can be whether chosen by users or set by PowerFLOW to a default Value. The Mach number $M=U/c_0$ is defined as the ratio of the characteristic velocity U to the speed of sound c_0 . For wind-noise cases or bluff-body type configurations, the characteristic velocity U is usually set as the mean velocity of the incoming flow, i.e. 40 m/s in this work.

The duration of the simulated flow is 1.2 second. The only difference in the numerical setup between the two simulations that we performed is the Mach number setting.

The simulated Mach number was first defined as ‘‘Same as experiments’’. The simulated variables, such as velocity and pressure, correspond then to the ones of a real wind-tunnel experiment performed at the characteristic flow speed U . In this type of calculation, so-called ‘‘Mach Matched’’ (MM), acoustic wave will propagate at the same speed relative to the main flow as they do in experiments, what should be more appropriate for further acoustical analysis. On the other hand, each time step corresponds to a smaller interval of physical time, so that we needed to run the simulation for a longer period of time (Table 1).

In order to reduce the calculation times by a factor R referred as the ‘‘Mach ratio’’, the simulated Mach number can be artificially increased to the value $R \times M$. For external wind-noise simulations, when the Mach number option ‘‘chosen by PowerFLOW’’ is used, the simulation Mach number is set to $M=0.315$ which is considered the maximum safe value for the incoming mean flow velocity. We performed our second simulation using this ‘‘Default Mach’’ number setting (DM). For this type of simulations, the turbulent flow variables are still accurately predicted but the apparent speed of sound waves is affected by a factor $1/R$.

The simulation details are given in Table 1. In the DM case, the Mach ratio was $R=2.7$, hence the simulation ran almost three times faster than in the MM case.

Table 1: simulations parameters

Mach number setting	Chosen by PowerFLOW (DM)	Same as Experiments (MM)
Simulated Mach	0.31497	0.1165
Time step (s)	4.455×10^{-6}	1.649×10^{-6}
Number of time steps	269343	727890
CPU time (hours)	1848.6	5241.5

3 Comparison with experiments

Before processing the computed WPF data, the numerical results have been validated by comparison with experiments. The measurements have been carried out at the CEAT (Centre d’Études Aérodynamiques et Thermiques, Poitiers, France) anechoic Eiffel-type wind-tunnel [3]. The WPF were measured using pinhole microphones at 32 locations in the wake of the side mirror (Figure 3).

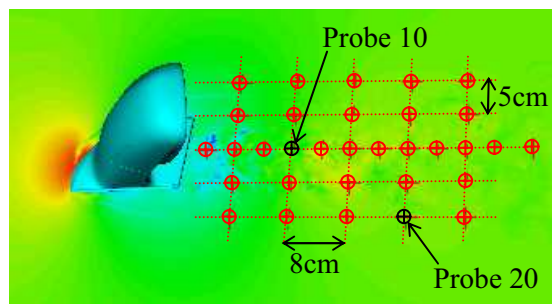


Figure 3: Probes’ location on the measurement floor

A good correlation between the measured and the computed PSD is observed in the middle of the wake, as shown for instance at probe n°10 on Figure 4. There is no difference between the two Mach number settings below 2 kHz. Above this frequency, the MM setting leads to an underestimation of the PSD while the DM setting allows a good correlation with the measured PSD up to 4 kHz.

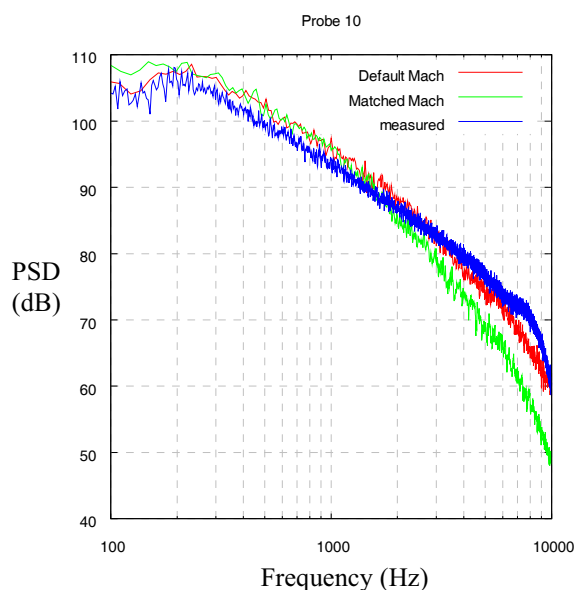


Figure 4: WPF PSD in the middle of the wake (probe n°10)

This difference might be cancelled by using a finer mesh for the MM mode, so that a fluid particle would cross the same number of voxels at each time step than a particle moving faster on a coarser mesh with the DM mode.

In the quiet zone outside the wake, the numerical prediction underestimates the measured PSD (Figure 5) above 1 kHz. This could be explained by a numerical prediction of a too narrow wake compared to the more widely spread real wake. Another explanation could be that the sensitivity of the microphones is too weak to correctly measure the WPF in the quiet zone. Since the WPF levels in that region are lower than in the critical reattachment zone, discrepancies in these quieter areas are anyway not very significant for the overall prediction quality.

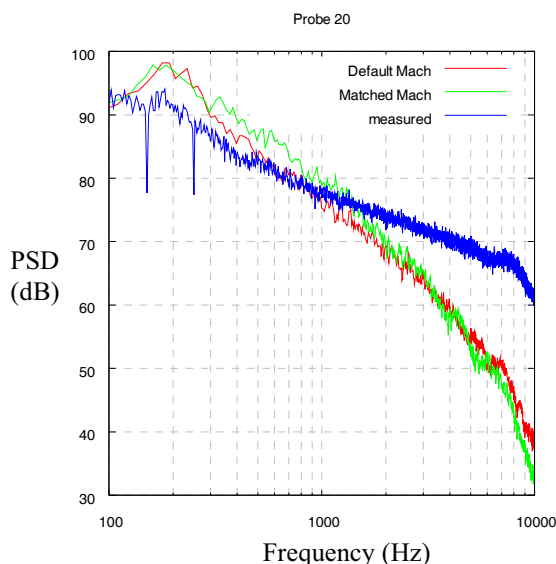


Figure 5: WPF PSD out of the wake (probe n°20)

4 Wavenumber Frequency analysis

The WPF is recorded on the measurement floor by averaging over regular time intervals in order to reduce the size of the data written to disk. The time between the centre of two successive averaging frames defines the period T and the sampling frequency $F_s=1/T$ of the stored WPF history. The time averaging parameters are given for both Mach number settings in Table 2.

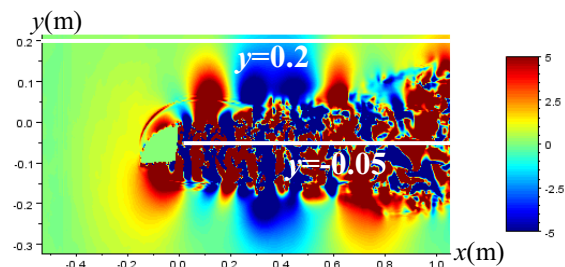
Table 2: time averaging

Frames' parameters	F_s (Hz)	Averaging time (s)	Number of Timesteps per frame	Number of frames
DM	20405	4.95×10^{-5}	11	20405
MM	20219	4.95×10^{-5}	30	20219

To achieve convergence of the calculations, the records started after 0.2s of physical time.

The k_x - ω diagrams of the WPF PSD are obtained using the averaged weighted periodogram's method described by Van Herpe et al. [3]. We averaged 8 periodograms computed over of 4096 frames weighted by a two dimensional Hanning window, with an overlap of 50%.

The diagrams presented in this paper correspond whether to the line $y=-0.05$ m (middle of the wake) or to the line $y=0.2$ m (outside the wake) as shown on Figure 6.

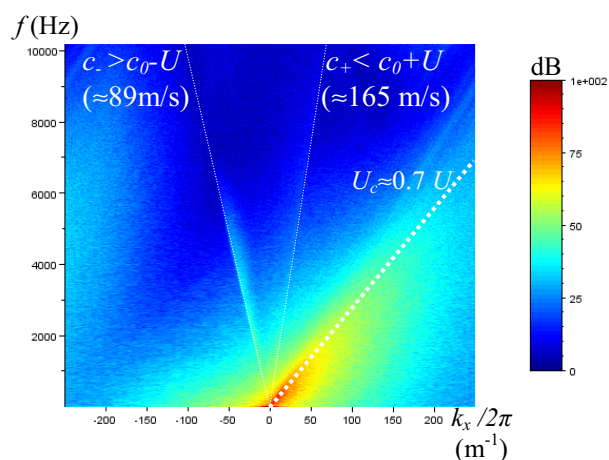
Figure 6: Position of the lines of constant y for space and time Fourier transform of the WPF

4.1 Default Mach setting (DM)

When the Mach number is “chosen by PowerFLOW”, the acoustic cone is clearly visible on the k_x - ω diagram of the WPF PSD, even in the middle of the wake (Figure 7) where the convective component is the strongest. This cone is not symmetrical about the $k_x=0$ axis because the flow speeds up the acoustic waves propagating downstream ($c_+ \leq c_0 + U$) and slows down the acoustic waves propagating upstream ($c_- \leq c_0 - U$). This is why the slope of the straight line limiting the acoustic cone on the right side ($k_x > 0$) is larger than the slope of the one limiting the cone on the left side ($k_x < 0$). The pseudosound component of the WPF lies as expected around the convection velocity line ($U_c \approx 0.7U$).

Outside the wake (Figure 8), only the propagating component of the WPF is visible inside the acoustic cone.

However, one can observe on those two diagrams that the magnitude of the acoustic waves propagating upstream ($k_x < 0$) is higher than the magnitude of those propagating downstream ($k_x > 0$). This could be explained physically by the directivity of the flow-induced noise source which would radiate more sound in the upstream direction, but the WPF animations have rather shown a reflection of the acoustic waves from the outlet boundary. We suppose that the sponge zones used to damp spurious reflections from the limit of the computational domain are not efficient enough. This question is still under investigation and further analyses are on-going.

Figure 7: k_x - ω diagram of the WPF PSD at $y=0.2$ m

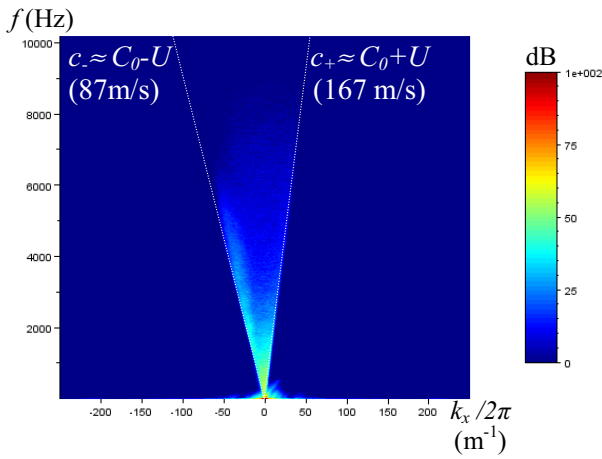


Figure 8: k_x - ω diagram of the WPF PSD at $y=0.2m$

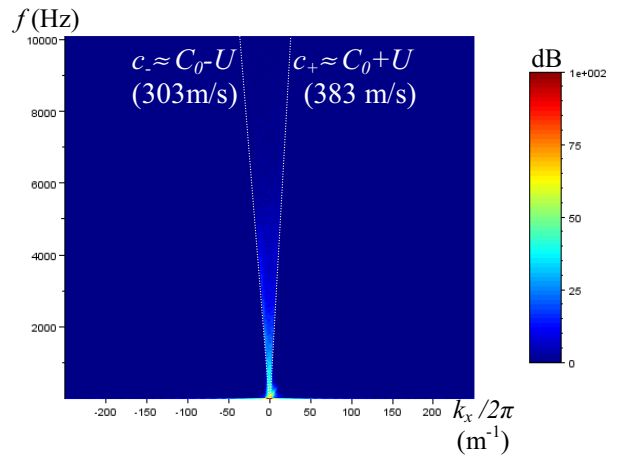


Figure 10: k_x - ω diagram of the WPF PSD at $y=0.2m$

4.2 Matched Mach setting (MM)

When the Mach number is the “same as experiments”, with the same colour scale as the previous k_x - ω diagrams (§4.1), one can hardly guess the acoustic cone in the middle of the wake (Figure 9). This means that the magnitude of the predicted acoustic component of the WPF is much lower than with the default Mach number.

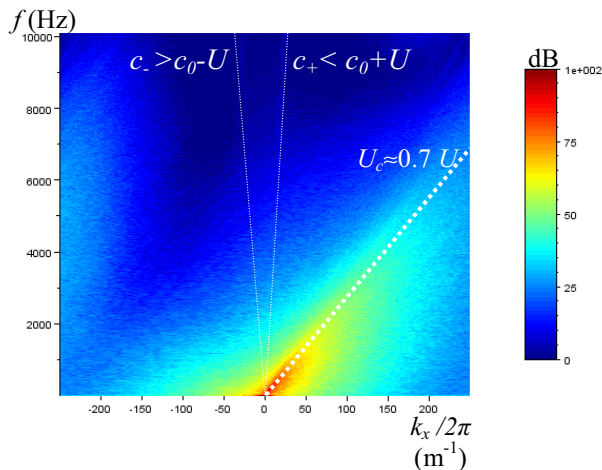


Figure 9: k_x - ω diagram of the WPF PSD at $y=-0.05m$

The acoustic component is however still captured, as shown by the diagram outside the wake (Figure 10). Nevertheless, it does not clearly emerge in the middle of the wake (Figure 9) because its magnitude is too weak relative to the amplitude of the convective component.

The magnitude of the acoustic component of the WPF seems to depend on the Mach number setting; this is what we quantify in next section.

4.3 DM vs MM

We compare in this section the magnitude of the WPF PSD at a given frequency as a function of the dimensionless number $k_x U / \omega$ for the DM and the MM settings. At 3 kHz, in the middle of the wake, Figure 11 shows that the magnitude of the incompressible part of the WPF, i.e. the convective peak lying around $k_x U_c / \omega = U / U_c$, depends as well on the Mach number setting. This phenomenon was already observed in §3 for frequencies greater than 2 kHz. This graph also confirms that the emergence of the acoustic component of the PSD ($U/c_- < k_x U / \omega < U/c_+$) is higher by more than 5 dB with the DM setting than with the MM one.

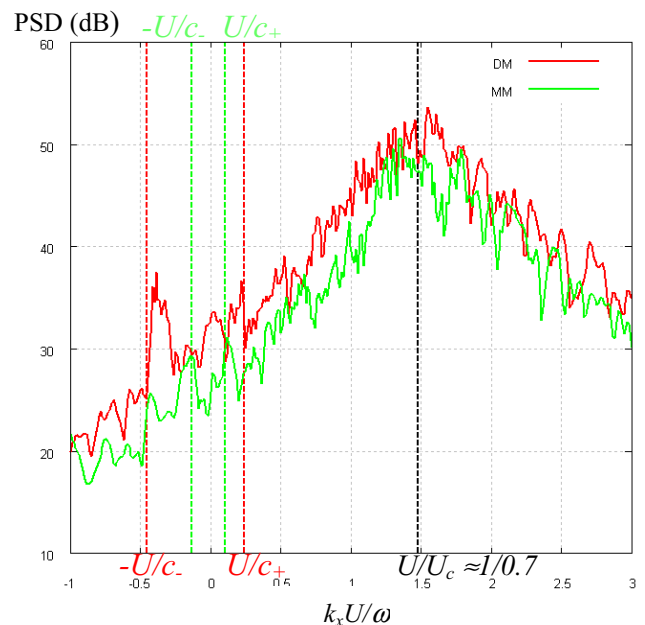


Figure 11: WPF PSD at 3000 Hz in the middle of the wake $y=-0.05m$

The difference is even more obvious and can reach more than 10 dB outside the wake (e.g. Figure 12 at 2 kHz), where the compressible sound field is not masked anymore by the incompressible pseudosound field.

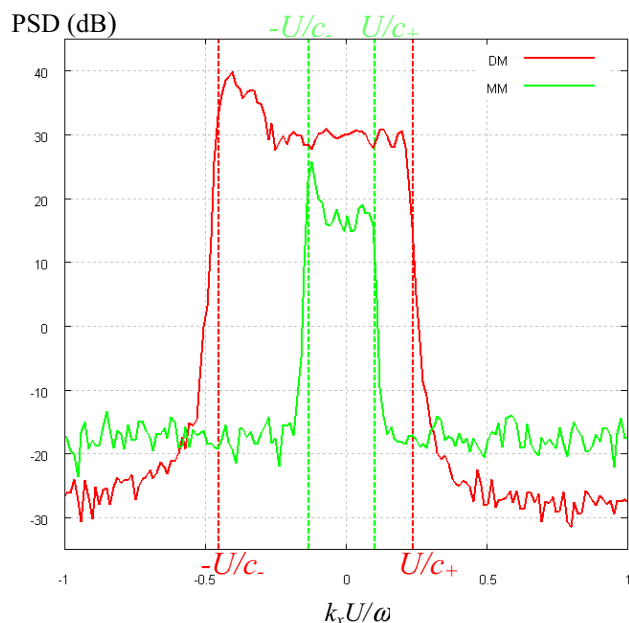


Figure 12: WPF PSD at 2000Hz outside the wake ($y=0.2m$)

5 Conclusion

This work confirmed that the Lattice Boltzmann based CFD code PowerFLOW is able to capture the low level acoustic compressible component of the WPF. We separated this acoustic component from the convective one using a wavenumber-frequency Fourier transform of the WPF.

We observed however that the magnitude of the acoustic component of the WPF depends on the Mach number setting. If we believe that this component has an important contribution to the wind noise inside the car cabin, the choice of the Mach number is then an important parameter for our computational aero-acoustic predictions. By default, PowerFLOW runs the simulation at a Mach number as high as physically possible. Without any further correction applied to the acoustic component, this choice might lead to an overestimation of the sound component of the WPF, probably because the higher Mach number chosen artificially enhances the intensity of the radiated sound.

It seems then more relevant for wind noise prediction to choose a Mach number matching the experimental one, so that the acoustic waves have the same magnitude as they do in experiments. However, this Mach number setting requires running the simulation for a much longer period of time: Each time step corresponds to a smaller interval of physical time and a finer mesh might also be needed for the same level of accuracy.

In practice, it would be necessary to know how the magnitude of the acoustic component of the WPF varies with the Mach number: One could then use the default Mach number setting to run more efficient calculations and correct the level of the acoustic component to match the level that one would obtain with the same Mach number as in experiments.

An interesting prospect would then be to run several simulations with different Mach number settings in order to observe how the intensity of the flow-induced sound component varies with the Mach number (M^α law?). This kind of approach has been carried out for instance in the case of automotive HVAC ducts and registers [4], and showed that the radiated acoustic power varies with the mass flow rate Q following a Q^α law.

Acknowledgments

The authors would like to thank Mohammed Meskine and Franck Perot from Exa Corporation, for their precious help to set up efficient calculations and to understand physically the numerical results.

References

- [1] P. G. Bremner, M. Zhu, "Recent Progress using SEA and CFD to Predict Interior Wind Noise", SAE paper 2003-01-1705
- [2] P. Moron, R. Powell, D. Freed, F. Pérot, B. Crouse, B. Neuhierl, F. Ullrich, M. Höll, A. Waibl, and C. Fertl, "A CFD/SEA Approach for Prediction of Vehicle Interior Noise due to Wind Noise", SAE paper 2009-01-2203
- [3] F. Van Herpe, M. Bordji, D. Baresh, P. Lafon, "Wavenumber-Frequency Analysis of the Wall Pressure Fluctuations in the Wake of a Car Side Mirror", AIAA paper 2011-2936
- [4] F. Pérot, M. Meskine, F. Gille, Sandrine Vergne, "Aeroacoustics prediction of simplified and production automotive HVAC ducts and registers", AIAA paper 2011-2935